Primitives extraction based on structured-light images

Vincent Daval, Frederic Truchetet, Olivier Aubreton

Primitives extraction based on structured-light images

Vincent Daval
Laboratoire Electronique
Informatique et Image
Le creusot, France, 71200
vincent.daval@u-bourgogne.fr

Fréderic Truchetet
Laboratoire Electronique
Informatique et Image
Le creusot, France, 71200
frederic.truchetet@u-bourgogne.fr

Olivier Aubreton
Laboratoire Electronique
Informatique et Image
Le creusot, France, 71200
olivier.aubreton@u-bourgogne.fr

***Abstract*—Geometric attributes such as curvature or surface orientation are additional information of the 3D points obtained after the scanning of an object. In the classic 3D chain, characterized by a sequential structure, these information are determined from the dense point cloud (from a 3D scanner). Then, they are used to reduce the amount of information and allows to obtain a simplified model. In this paper, we investigate the possibility to extract some geometric attributes, directly from 2D images obtained by the camera of a structured-light system.**

Keywords—curvature; surface orientation; discontinuity; 3D reconstruction; structured light.

I. INTRODUCTION

Today, classic 3D chain appears as sequential and interactions between the various steps (acquisition, meshing and compression) are rarely studied. Actual scanning systems allows to obtain a point cloud of several million points, while the successive operations that lead to a simplified model (compressed or modelled by primitives) try to reduce the amount of data. In addition, many of these methods are based on curvature estimation and/or surface orientation for each 3D point. However these operators are generally suitable for smoothed dense meshes. They are costly in resources and computing time.

The Creactive project is a collaborative work between three partners: the company Noomeo [1] specialized in the development of 3D scanning solutions, I3S [2] whose some members are interested by 3D compression of data and the 3D Vision team of LE2I [3]. The objective of this project is to investigate the possible interactions between the different parts of the classic 3D chain and the development of a structured-light system facilitating the operations permitting to obtain a compressed model or modelled by primitives (CAD for example).

This project is composed of two parts. The first part consist to extract different attributes during the acquisition (orientation, curvatures, discontinuities, primitives) in order to guide the operator (in red in Fig. 1). The aim of the second part is to pilot the acquisition process by extracting information from the mesh (in green in Fig. 1). The first part is developed by the laboratory LE2I and the second by the laboratory I3S. This paper concerns the first part of the project.

Generally, the different steps of the 3D chain are treated separately by different operators, each of them with different skills. Acquisition involves skills in vision, meshing/compression in signal processing, and surface reconstruction (for reverse engineering and surface inspection) in mechanic. The classic approach consist to acquire a lot of views to allow at the vision operator to obtain a good CAD model. However, in some cases it is not necessary to acquire as many scans to compute a good CAD model (corresponding to requirements established). The primitives extraction during acquisition could guide the vision operator to minimize the number of views, facilitating the meshing/surface reconstruction.

In this article, we focus on the extraction of additional attributes to 3D points, such as surface orientation at each point (II), local curvature (III) or surface discontinuity (IV). The use of these attributes and the perspectives of results will be discussed in the conclusion (IV).

II. SURFACE ORIENTATION EXTRACTION

Currently, there are different methods to extract geometric information, during acquisition, as for 3D orientation. For example "Shape from Shading" that requires the knowledge of the reflectance map of the surface [4], "Shape from polarization" [5], deflectometry [6] and "Scanning from heating" [7]. These methods are only applicable on specular/transparent surface.

In the case of diffuse surfaces (that approach a Lambertian behavior), scanning system by active triangulation are perfectly adapted. The principle has been extensively studied in recent years. Spatial encoding patterns [8-11], facilitate the matching with the acquired images and require only one projection. In addition, as authors have presented in [12], the use of particular pattern permits a determination of the surface orientation at each point from the analysis of the acquired images. However, they remain sensitive to the texture of the object. The use of temporal encoding patterns [13-16] permits to improve the robustness but require the projection of an image sequence. However, the forms of the used pattern (alternating black and white stripes) do not allow to extract surface orientation.

As show on Fig. 2, a binary grid is associated with a pattern sequence in a gray code. Thus, at each point (line intersections) correspond a unique coding using the projection of temporal encoding. We chose to combine the temporal encoding approaches with the method proposed in [12].

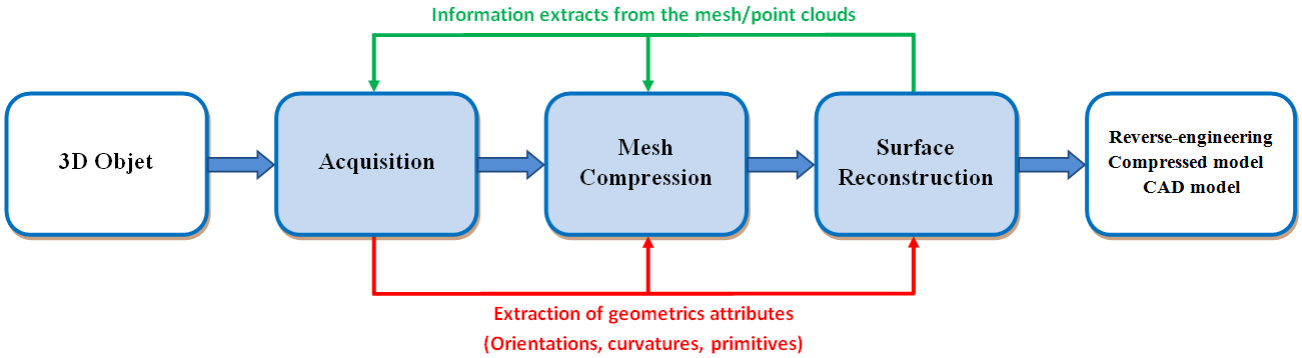

Fig. 1: *Classic 3D chain. In red and green, the contributions of the project.*

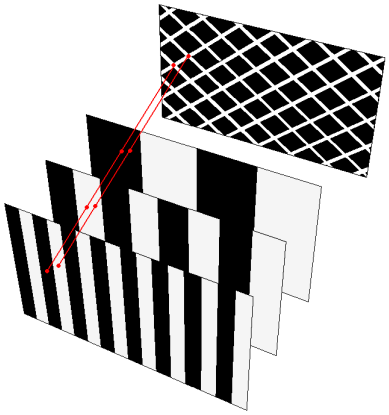

Fig. 2: *Illumination pattern and encoding used.*

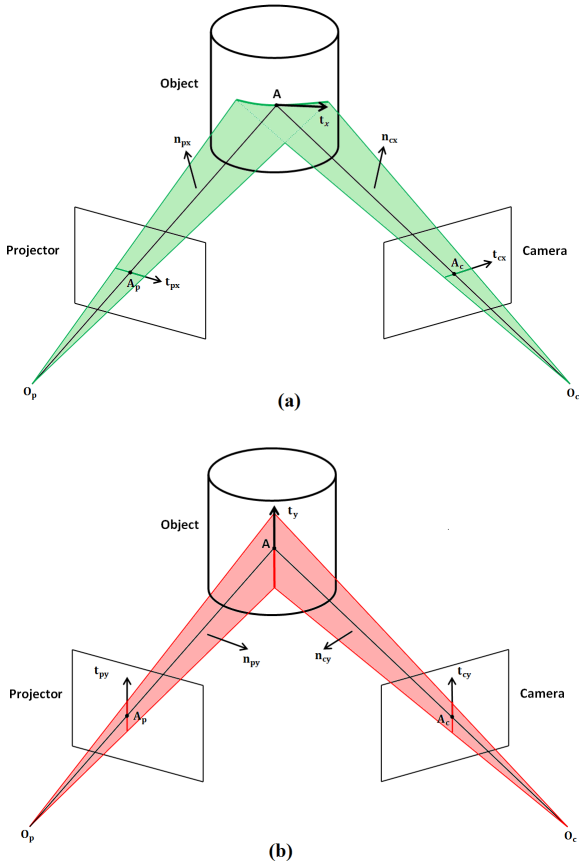

Fig. 3: *Principle used to compute the surface orientation.*

A. *Principle of surface orientation determination*

With the same method, presented by the authors in [12], consider any point on the projector grid A_p. This point is composed of two grid lines, as illustrated by Fig. 3 (in red and green on the Fig. 3). The projection of this point on the surface of a 3D object give a point A. The capture of A by the camera gives a point A_c on the image camera. We note the tangents to the grid lines at point A_p: t_{px} and t_{py}, and to the grid lines at point A_c: t_{cx} and t_{cy}.

The tangent t_{px} and the center of the projector O_p form the lighting plane $\Pi(A_p, t_{px})$. This plane is reflected by the surface of the object at the point A and becomes the projection plane $\Pi(A_c, t_{cx})$ to the image plane. The intersection of both planes $\Pi(A_p, t_{px})$ and $\Pi(A_c, t_{cx})$ defines one tangent t_x at the surface of the object at the point A. A_p and t_{px} are known because it's the projected pattern. Similarly, A_c and t_{cx} are accessible from image observations. Knowing all data, it is possible to reconstruct both these planes $\Pi(A_p, t_{px})$ and $\Pi(A_c, t_{cx})$ and determine the intersection t_x.

Similarly, it is possible to compute another tangent t_y at the point A from two other planes $\Pi(A_p, t_{py})$ and $\Pi(A_c, t_{cy})$ which are constructible too. In other words, the proposed method in [12] permits to determine the surface orientation $n(x, y)$ of the object associated to the 3D point A, simply by looking at the surface illuminated by a known pattern. The 3D tangents t_x and t_y can be calculated, and the orientation of the surface is simply:

$$n(x, y) = t_x \times t_y. \tag{1}$$

We also note that the projected pattern is a regular grid. So, tangents t_{px} and t_{py} are known and are the same for all points of the grid.

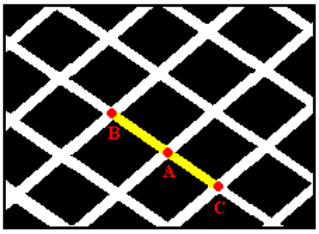

Fig. 4: *Tangent computation.*

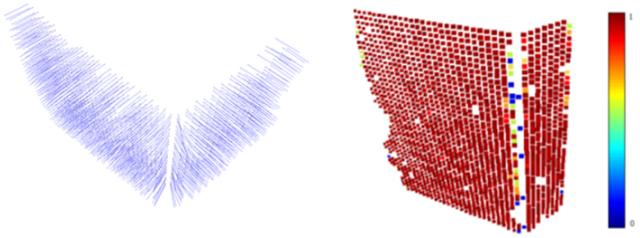

Fig. 5: *Results obtained by our approach. (a) Surface orientation map. (b). Angle between the orientation calculated and the orientation measured. The value is 1 when the angle is null and 0 when the angle is superior at 15°.*

B. Tangents detection

In this part, we describe how we extract the tangents from the image. We have reimplement the method proposed in [12] with own our pattern. Supposing we want to compute the tangent t_{cx} at point A. The Fig. 4 shows t_{cx} as two grid lines segments (in yellow). As show in Fig. 4, along the line associated to A, there are two adjacent points B and C. The image tangent t_{cx} at point A can be determined as a good approximation by a simple finite difference between B and C.

C. Orientation estimation

We note n_{cx} and n_{cy} the normal vectors to the planes $\Pi(A_c, t_{cx})$ and $\Pi(A_c, t_{cy})$ associated to the camera, and n_{px} and n_{py} the normal vectors to the planes $\Pi(p_p, t_{p1})$ and $\Pi(p_p, t_{p2})$ associated to the projector. The system being calibrated, the intrinsic parameters of the camera and the projector are known. These parameters are the focal distances f_c, f_p and the principal points, respectively $C_c(x_{c0}, y_{c0})$ and $C_p(x_{p0}, y_{p0})$. Using these parameters, the four normal at the planes n_{cx}, n_{cy}, n_{px}, n_{py} can be determined as follows:

$$\overrightarrow{n}_{cx} = p_c \times \begin{bmatrix} t_{cx} \\ 0 \end{bmatrix}, \quad \overrightarrow{n}_{px} = p_p \times \begin{bmatrix} t_{px} \\ 0 \end{bmatrix}, \tag{2}$$

$$\overrightarrow{n}_{cy} = p_c \times \begin{bmatrix} t_{cy} \\ 0 \end{bmatrix}, \quad \overrightarrow{n}_{py} = p_p \times \begin{bmatrix} t_{py} \\ 0 \end{bmatrix}, \tag{3}$$

where $p_c = [(x_c - x_{c0}), (y_c - y_{c0}), f_c]^T$, $p_p = [(x_p - x_{p0}), (y_p - y_{p0}), f_p]^T$ and with $(x_c, y_c), (x_p, y_p)$, respectively the positions of the grid points for the camera and for the projector. The two 3D tangents t_x and t_y at point A are:

$$t_x = n_{cx} \times (Rn_{px}), \quad t_y = n_{cy} \times (Rn_{py}), \tag{4}$$

where R is the rotation between the camera and the projector. Finally, the surface orientation at point P can be determined by:

$$n(x, y) = t_x \times t_y \tag{5}$$

D. Results

Our structured light system is composed of a camera (resolution 1280×1024) and a projector (resolution 1024×780).

To extract 3D points and different geometrical information (orientation curvature, discontinuities), the system must be calibrated. The camera calibration has been heavily studied and there are many techniques to calibrate a camera, including for example [17] and [18]. If the camera calibration techniques are now widespread, there are significantly fewer techniques used to calibrate the projector-camera system. We can point out two of them: [19] and [20].

The method presented in [20] gives very good results both for camera calibration and projector calibration. For this reason, we have chosen to calibrate our system by applying this method.

The results obtained on a cube (Fig. 5) shows the angle between the orientations calculated on the point cloud by the software RapidForm and those measured using our method.

We see, on this result, that the measured orientations are very similar to calculated normals excluding the orientations located at the edges of the cloud, where the error is quite large.

III. Curvature evaluation

As we have just seen, there are different approaches to extract the orientation at each point in the 3D acquisition using structured light. However, some geometric attributes (such as curvature) are not much used although they carry information. We have used a similar approach, based on the analysis of the patterns observed in the images, in order to determine the local curvature of the surface of the object. In this section we present a new approach permitting to estimate a directional curvature of an object from the same pattern as presented previously.

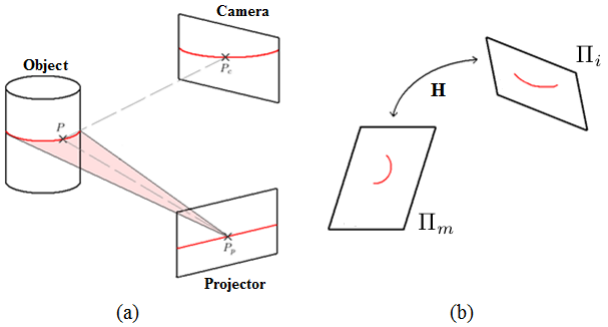

Fig. 6: *Program of the problematic. (a) Principe used to determine the curvature. (b) Relation between the lightning plane (half circle) and the image camera plane (half ellipse).*

Projecting a line with a projector, we generate a lightning plane Π_m. This plane intersect the 3D object.We take a particular case: a cylinder. As illustrated by the Fig. 6, this intersection is a half circle in the plane Π_m (if the lightning plane is perpendicular to the cylinder axis). The visualisation of the scene by the camera form a half ellipse in the plane of the camera's image plane Π_i. This problem can be simulated by the projective transformation of a conic (which is the general form of an ellipse) between the planes Π_m and Π_i.

The relationship between two spaces of the same dimension, in fact, the planes Π_m and Π_i, is a particular matrix classically called Homography. Generally, for two points X_i and X_i' appertaining respectively to Π_m and Π_i, we have:

$$X_i' = HX_i. \tag{6}$$

As explained previously, this problem can be seem as the projective transformation of a conic A_Q between the plane Π_m and Π_i. We note the new resulting conic A_Q'. The matrix H permits to transfer the conic between the planes Π_m and Π_i. Take a point $q = (x, y, 1)^T$ appertaining to the plane Π_i and its projection $q' = (x', y', 1)^T$ appertaining to the plane Π_m. Using the definition of a conic, we can write:

$$q^T.A_Q.q = 0, \tag{7}$$

we know

$$q' = H.q, \tag{8}$$

we search A_Q' such as:

$$q^{'T}.A_Q'.q' = 0. \tag{9}$$

$$(H^{-1}Hq)^T.A_Q.H^{-1}Hq = 0, \tag{10}$$
$$(H^{-1}q')^T.A_Q.H^{-1}q' = 0, \tag{11}$$
$$q^{'T}H^{-T}.A_Q.H^{-1}q' = 0, \tag{12}$$
$$q^{'T}.A_Q'.q' = 0. \tag{13}$$

So we obtain

$$A_Q' = H^{-T}.A_Q.H^{-1}. \tag{14}$$

A_Q is can be deduced using the camera's image plane. If we know H, by another calibration step, it is possible to compute the conic A_Q' in the plane Π_m.

A. Parameters extraction

The resulting matrix of the projective transformation, A_Q' can be write in this following quadratic form Q:

$$Q = A'x^2 + B'xy + C'y^2 + D'x + E'y + F' = 0, \tag{15}$$

or

$$Q = \begin{bmatrix} A' & B'/2 & D'/2 \\ B'/2 & C' & E'/2 \\ D'/2 & E'/2 & F' \end{bmatrix}. \tag{16}$$

From this matrix, it is possible to extract different parameters as the center of the conic section in the plane Π_m or the radius of curvature. In fact, it is possible to extract the reduced equation of the circle and estimate the radius of curvature. Note λ_1 and λ_2 the eigenvalues of the sub-matrix A_{33}' with

$$A_{33}' = \begin{bmatrix} A' & B'/2 \\ B'/2 & C' \end{bmatrix}. \tag{17}$$

The reduce equation can be written:

$$\lambda_1 x'^2 + \lambda_2 y'^2 + \frac{detA_Q'}{detA_{33}'} = 0, \tag{18}$$

with x' and y' the position of a point on the curve (plane Π_m). Dividing by $-\frac{detA_Q'}{detA_{33}'}$, we can write:

$$\frac{x'^2}{r^2} + \frac{y'^2}{r^2} = 1. \tag{19}$$

By identification, we can extract the curvature radius r of the circle:

$$r = \sqrt{-\frac{detA_Q'}{\lambda_1 detA_{33}'}} \tag{20}$$

Object	radius measured by calliper	radius estimated by our method
Cylindre 1	4,50 mm	4,37 mm
Cylindre 2	3,45 mm	3,41 mm
Cylindre 3	2,82 mm	2,75 mm

TABLE I: *Results obtain by our method on three cylinders.*

real radius	radius estimated with 100 points	radius estimated with 50 points	radius estimated with 20 points
4,50 mm	4,37 mm	4,85 mm	6,2 mm
3,45 mm	3,41 mm	3,65 mm	4,52 mm
2,82 mm	2,75 mm	2,74 mm	3,80 mm

TABLE II: *Results obtain by our method depending to the number of points used to determine the conic A_Q.*

B. Results

The Tab. I shows examples of calculated curvature with our system on several cylinders of different diameters, measured with a calliper. For these three examples, we obtain a maximum radius error of 3% to the real curvature radius. However, the quality of obtained results is highly dependent of the number of points used to perform the estimation of the conic on the image camera, as shown in Tab. II.

This approach is limited to surfaces with a consequent size. It is not adaptable in to important curvature and more particularly in the case of the object presented discontinuities.

IV. Discontinuities detection

In this part, we propose a method permitting to detect discontinuities in one particular direction from images (using the same pattern as before).

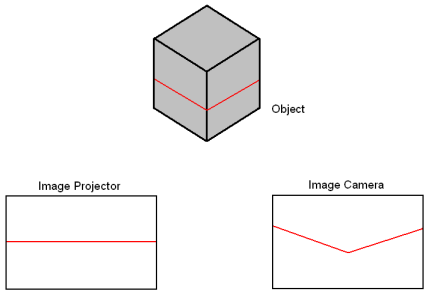

Fig. 7: *Deformation of the projected line on the object.*

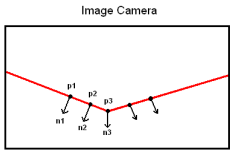

Fig. 8: *Principle of our discontinuities detector.*

A. Principle

As the previous case, we consider only one line of our pattern. As illustrated by the Fig. 7, a discontinuity of the 3D object can be visualized from the image camera. This discontinuity can be detected measuring a local variation of the normals at this line (Fig. 8).

In our practical case, these normals are the normals vectors to the tangents line previously calculated. Calculating the variation of this normals, along the line it is possible to estimate the localisation of the discontinuities.

B. Results

The Fig. 9-b and Fig. 10 show several results of our approach. To test our method, we have use the object presented in Fig. 9-a an in Fig. 12-a. This object is composed by several planes with sharp edges between each planes. On these examples, the edges appear well localized. A retro-projection on the real form (Fig 11) permits to verify the conformity of our discontinuities detector with the real shape of the object.

V. Conclusion

In this paper, we have presented several approaches which permit to determine additional attributes at the 3D point: surface orientation, directional curvature, discontinuity. The obtained results offer different perspectives, in particular concerning the segmentation of the analyzed shape and the identification of the different objects.

The detection of areas with an important curvature permits to consider specific scanning strategies such as "coarse to fine". A first coarse scan (low dense) allows a coarse detection of areas carrying information. These areas could be scan another time, a finer scan, by acting on the projected pattern.

Another application is the modeling of the objet from basic primitives. From the geometric attributes determined from im-

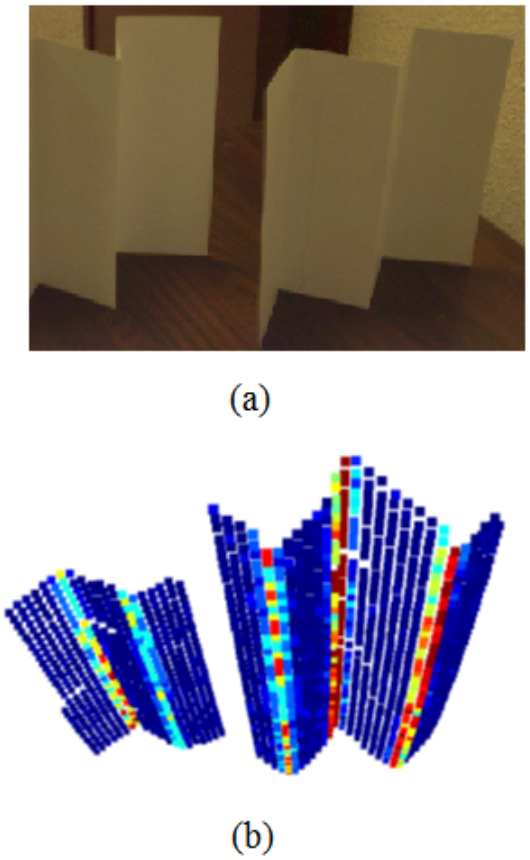

Fig. 9: *Results obtained on a test object. (a) The test object. (b) Results: in blue, no discontinuities, probably plane object. In red, important discontinuities, probably a sharp edges.*

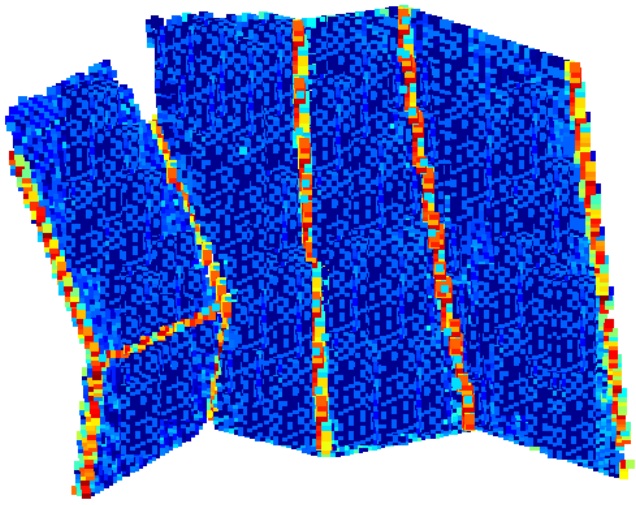

Fig. 10: *Result of our discontinuities detector on the object presented in Fig. 12-a.*

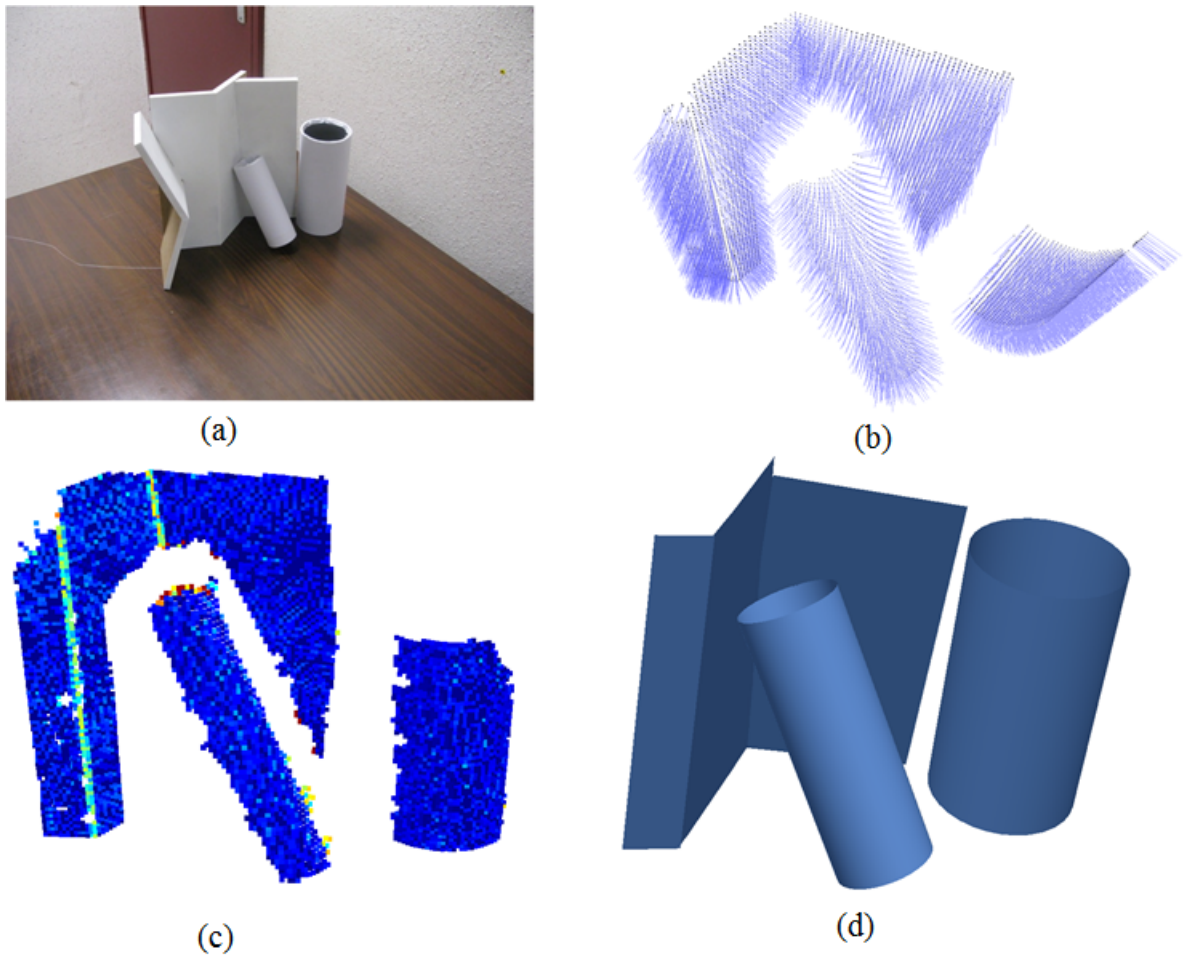

Fig. 12: *Primitives extraction. (a) Test object composed of planes and cylinders. (b) Surface orientations map. (c) Discontinuities map. (d) Modeling primitives.*

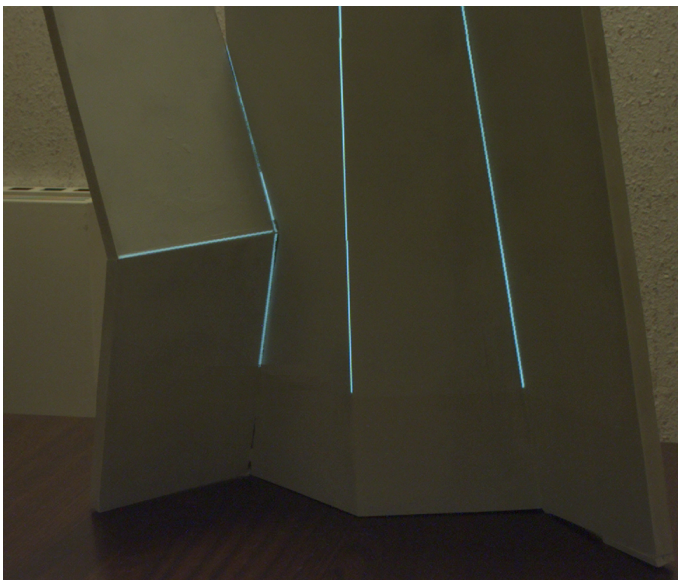

Fig. 11: *Verification of localization of edges with our approach, by reprojection on the object.*

ages, the different elements of the object can be differentiated, segmented and represented by planes, cylinders...

An example of result, from preliminary test, is presented in Fig. 12. Surface orientations discontinuities and curvatures, necessary to determine primitives (planes and cylinders), are obtained per the solutions presented in this paper.

REFERENCES

[1] Société Noomeo, *http://www.noomeo.eu/,* Labege, France.

[2] Laboratoire d'Informatique, Signaux et Systèmes de Sophia Antipolis, *http://www.i3s.unice.fr/I3S/,* Sophia Antipolis, France.

[3] Laboratoire Électronique Informatique et Image, *http://le2i.cnrs.fr/,* Le creusot, France.

[4] R. Zhang, P. Tsai, J. E. Cryer, M. Shah, *Shape from shading : A survey,* IEEE Transactions on Pattern Analysis and Machine Intelligence, 21(8) :69-0706, 1999.

[5] O. Morel, C. Stolz, F. Meriaudeau, P. Gorria, *Active lighting applied to 3d reconstruction of specular metallic surfaces by polarization imaging,* Applied Optics, 45 :4062-4068.

[6] Y. Surrel, *Mesure et contrôle de planéité par déflectométrie,* Contrôle et mesures optiques pour l'industrie, pages 271-275, 2004.

[7] G. Eren, *3D scanning of transparent objects,* thesis report, Université de Bourgogne; Turquie - Université de SABANCI, 2010.

[8] S. Kiyasu, H. Hoshino, K. Yano, S. Fujimura, *Measurement of the 3-D Shape of Specular Polyhedrons Using an M-Array Coded Light Source,* IEEE Trans. Instrumentation and Measurement, vol. 44, no. 3, pp. 775-778, June 1995.

[9] P. Griffin, L. Narasimhan, S. Yee, *Generation of Uniquely Encoded Light Patterns for Range Data Acquisition,* Pattern Recognition, vol. 25, no. 6, pp. 609-616, 1992.

[10] J. Salvi, J. Batlle, E. Mouaddib, *A Robust-Coded Pattern Projection for Dynamic 3D Scene Measurement,* Pattern Recognition Letters, vol. 19, pp. 1055-1065, 1998.

[11] R.A. Morano, C. Ozturk, R. Conn, S. Dubin, S. Zietz, J. Nissano, *Structured Light Using Pseudorandom Coded,* IEEE Trans. Pattern Analysis and Machine Intelligence, vol. 20, no. 3, pp. 322-327, Mar. 1998.

[12] Z. Song, R. Chung, *Determining both surface position and orientation in structured-light-based sensing,* IEEE Transactions on Pattern Analysis and Machine Intelligence, 32: 1770-1780, 2010.

[13] I. Ishii, K. Yamato, K. Doi, T. Tsuji, *High-Speed 3D Image AcquisitionUsing Coded Structured Light Projection,* Proc. Int'l. Conf. Intelligent Robots and Systems, pp. 925-930, 2007.

[14] I .SR. J. Valkenburg, A. M. McIvor, *Accurate 3D Measurement Using a Structured Light System,* Image and Vision Computing,vol. 16, no. 2, pp. 99-110, 1998.

[15] W. Krattenthaler, K.J. Mayer, H.P. Duwe, *3D-Surface Measurement with Coded Light Approach,* Proc. 17th Meeting Austrian Assoc. for Pattern Recognition on Image Analysis and Synthesis, pp. 103-114, 1994.

[16] S. Zhang, P.S. Huang, *High-Resolution, Real-Time Three-Dimensional Shape Measurement,* Optical Eng., vol. 45, no. 12, p. 123601, 2006.

[17] Z. Zhang, *A flexible new technique for camera calibration,* IEEE Transactions on Pattern Analysis and Machine Intelligence, 22:1330-1334, 1998.

[18] R. Tsai, *An efficient and accurate camera calibration technique for 3d machine vision,* Proceedings of IEEE Conference on Computer Vision and Pattern Recognition, 0 :pp. 364-374, 1986.

[19] Z. Song and R. Chung, *Use of LCD Panel for Calibrating Structured Light-Based Range Sensing System,* IEEE Trans. Instrumentation and Measurement, vol. 57, no. 11, pp. 2623-2630, Nov. 2008.

[20] S. Audet, M. Okutomi, *A user-friendly method to geometrically calibrate projector-camera systems,* Computer Vision and Pattern Recognition Workshop, 0 :47-54, 2009.